Pseudo-atom calculation of energetics in metals

Pseudo-atom calculation of energetics in metals

Robert W Jansen and Barry M Klein

Complex Systems Theory Branch, Naval Research Laboratory, Washington, DC 20375-5000, USA

Abstract. A mixed-basis approach for calculating first-principles electronic structure and total energies in metals is presented. The technique uses the local-density approximation for exchange and correlation in the pseudopotential framework and a minimal basis of localised pseudo-atomic orbitals which may be supplemented with a few low-energy plane waves. Aside from being accurate, the method is faster and the results are more easily interpretable than conventional plane-wave methods. The method is used to calculate bulk properties of Al and Nb and the vacancy and high-symmetry octahedral-site self-interstitial formation energies in Al.

1. Introduction

Ab initio orbital-based methods have received much interest for electronic structure calculations in condensed systems since they provide a simple interpretation of bonding in solids and they make feasible calculations involving large systems if the basis is kept relatively small [1–9]. Unfortunately, the determination of optimum minimal orbital basis sets can be a tedious and time-consuming task often requiring the sampling of several sets of functions before a suitable basis set is determined. Furthermore, the set-up of the Hamiltonian and overlap matrices requires the evaluation of numerous multi-centre integrals which can severely limit the form of the analytic functions which may be easily employed as basis functions—normally to only Gaussian type.

One way of circumventing the need for testing various sets of basis functions is to utilise the results of atomic calculations. If one can view the solid state wavefunction as only a small perturbation from a periodic array of overlapping atomic wavefunctions, then a basis set consisting of the atomic orbitals should represent a highly optimum spanning set for the solid state wavefunction. In many solids, however, particularly metals, the wavefunction contains highly disturbed free-electron-like components which are not easily represented by a few localised atomic orbitals. If a purely localised orbital basis is to be used for such materials, one often finds that several orbitals from excited atomic states with higher principal or angular momentum quantum numbers are needed to give an accurate characterisation of the charge density. Thus, the advantage in computational speed of a minimal-orbital-based method over the more rigorously complete basis-set methods, such as the linearised augmented plane-wave [10] method or the conventional plane-wave-based pseudopotential [11] method, is easily lost in such systems.

In this paper a method which incorporates a minimal basis of pseudo-atomic orbitals (PAOs) in the self-consistent pseudopotential scheme [11] is used to compute the electronic structure, total energies and defect formation energies of metals. The method is fast in the spirit of a linear muffin-tin orbital [12] or augmented spherical-wave [13] approach but avoids the approximations inherent in the use of a muffin-tin potential. To account for free-electron-like components in the wavefunction properly, while avoiding the use of a large number of orbitals, we also chose to supplement the PAO basis with a few low-energy plane waves. Thus our basis is composed of both localised (PAOs) and delocalised (plane waves) functions. For insulating and semiconducting systems, satisfactory results were found [1,2] for a variety of problems; these could be obtained even with just sp^3 PAOs and no plane waves. For metallic systems, we find the mixture of a few low-energy plane waves with the PAOs forms a nearly ideal basis and has significant advantages over the more conventional plane-wave-based pseudopotential method. The method is computationally efficient and allows for systematic improvements in the accuracy of the calculation, if desired. The resulting wavefunctions, which are sums of atomic orbital components, are also more easily interpreted than conventional plane-wave-based calculations where the wavefunctions are simply large Fourier sums. The outline of the paper is as follows. In § 2, we briefly describe the method. Section 3 will give some results for bulk properties of Al and Nb. In § 4, we calculate the formation energies for the vacancy and the self-interstitial in Al. We consider only the highest-symmetry interstitial site which is located at the centre of the face-centred cubic (FCC) cube. This interstitial site has six-fold coordination (octahedral symmetry) and is expected to be the lowest-energy interstitial site. Section 5 concludes.

2. Method

The method that we use is similar to a tight-binding-like approach but is based completely on first principles, requiring no adjustable parameters. We use the local-density approximation (LDA) within the self-consistent pseudopotential scheme. The pseudopotentials are of the type in [14] and were fitted to the form in [15]. We use the parametrisation in [16] of the exchange–correlation potential in [17]. The method is similar to earlier work in [3] but relies on PAOs constructed directly from the pseudopotentials. It has been described in detail and tested extensively for semiconductors in a previous publication [1]. Here we give only a brief outline of the method and investigate its applicability to metals.

Taking literally the tight-binding concept of the solid, we assume that a linear combination of Bloch functions of pseudo-atomic orbitals will form a close approximation to the true crystal wavefunction. As a starting point, we thus construct Bloch basis states for wavevector k and orbital μ (μ includes both the basis atom at τ and the s, or d orbital) by writing

$$\Phi_\mu(k, r) = \frac{1}{\sqrt{N}} \sum_l \exp[ik . (l + \tau)] \Phi_\mu^{PAO} (r - l - \tau) \qquad (1)$$

where l are the Bravis lattice sites. The expression for the Bloch states is identical with that used in the empirical tight-binding method, but here the orbitals $\Phi_\mu^{PAO}(r)$ are explicitly constructed from the atomic pseudopotentials for the isolated atoms using the same LDA as the solid. The electronic configurations used to produce the PAOs were the same as those used in the construction of the corresponding pseudopotentials.

Specifically, the ground-state orbitals were constructed from the ground-state atoms, while the excited-states orbitals (d for Al and p for Nb) were constructed from the excited configurations $s^1p^{0.75}d^{0.25}$ for Al and $d^3s^{0.75}p^{0.25}$ for Nb. The determination of the basis functions thus requires no 'guesswork' and can be constructed in parallel with (or otherwise obtained from) the pseudopotentials and fitted to analytic functions. Here we have chosen to use Slater orbitals as fitting functions, rather than Gaussians, since they better represent the wavefunction tails and effectively decay more rapidly in momentum space[†].

To facilitate simple evaluation of matrix elements, charge densities and total energies, we expand the PAOs into their Fourier components and work in the formalism of plane waves. Thus the PAOs are written as a sum over reciprocal lattice vectors g:

$$\Phi_\mu(k, r) \simeq \frac{1}{\sqrt{V}} \sum_{g(<g_2)} C_\mu(k - g) \exp[i(k - g) . r]. \tag{2}$$

The coefficient $C_\mu(k - g)$ is determined to be

$$C_\mu(k - g) = (1/\sqrt{v_c}) \exp(ig \cdot \tau) \Phi_\mu^{PAO}(k - g)$$

where v_c is the unit-cell volume and $\Phi_\mu^{PAO}(k - g)$ is the Fourier transform of the pseudo-atomic orbital. The approximate symbol in equation (2) becomes an equality as the energy cut-off E_2 ($E_2 = \hbar^2|k - g_2|^2/2m$) is taken to infinity. The cut-off E_2 in this method is similar to the cut-off used in the more conventional plane-wave-based calculations.

The Fourier decomposition of the wavefunction given by equation (2) is a computational convenience which, in addition to eliminating the need for evaluating explicit multi-centre integrals, allows one the flexibility of employing any functions which have convenient analytic Fourier transforms (such as Slater-type functions) as fitting functions for the PAOs. An additional advantage of this decomposition is that it allows for a straightforward means of improving the accuracy of the method if desired, by excluding a few low-energy plane waves in equation (2) and supplementing the local orbital basis by these excluded low-energy plane waves[†]. Thus, the crystal wavefunction is decomposed into a mixed basis of free electron-like low-energy plane waves and localised PAOS:

$$\Psi_k(r) = \sum_{g<g_1} a_k(g)\chi_g(k, r) + \sum_\mu b_k(\mu)\Phi_\mu'(k, r) \tag{3}$$

where $\chi_g(k, r) = (1/\Omega) \exp[i(k + g) \cdot r]$ and $\Phi_\mu'(k, r)$ is given by equation (2), but excluding the terms $g < g_1$[‡]. The variational coefficients $a_k(g)$ and $b_k(\mu)$ are self-consistently determined by solving $H\Psi_k = \varepsilon(k)S\Psi_k$, where H and S are the Hamiltonian and overlap operators.

The total energy is obtained using the formalism in [11] and can be expressed as

$$E_{tot} = \sum_k \eta_k \varepsilon_k + \sum_g F(g) + C \tag{4}$$

where η_k is the occupation number for the state k with eigenvalue ε_k, $F(g)$ includes the Fourier transform of the Hartree and exchange–correlation energy and C is a constant which includes ion–ion interactions and is independent of electronic structure.

† In the tail region the Gaussian transform will eventually decay more rapidly than the Slater transform, but at this crossover point the Slater orbital transform is only 10^{-3} its value at $g = 0$.

‡ Thus by construction, the PAOs are orthogonal to the low-energy plane waves. Numerical problems associated with an over-complete basis are in this way also avoided.

By keeping g_1 small in equation (3) the Hamiltonian matrix can be made far smaller than plane waves alone would allow. Since the diagonalisation time increases as the cube of the matrix dimension, this reduction in matrix size can lead to drastic reductions in diagonalisation time. Of course, the expansion of the PAOs in plane waves does lead to some increase in the time required for the set-up of the Hamiltonian, but this set-up time goes up only as N (not N^3), where N is the number of plane waves used in the expansion, and is therefore not a serious handicap. In supercell calculations, in fact, a number of simplifications become possible in the PAO approach which often leads to a reduction in the PAO set-up time over the plane-wave set-up time. For example, the time-consuming non-local potential only needs to be evaluated for each atom type and then multiplied by a phase factor. Generally the PAO approach is overall from three to 20 or more times faster than pure plane-wave pseudopotential calculations and is far more physically appealing. We have found no case where it is slower than plane waves for similar accuracy.

3. Bulk properties

To demonstrate the accuracy and versatility of the PAO method, we have computed a number of bulk properties for the simple FCC metal Al and the body-centred cubic (BCC) transition metal Nb. The calculations were done using a mesh of 20 special k-points in the irreducible (one-forty-eighth) Brillouin zone for both Al and Nb. The expansion in equation (2) was taken out to a kinetic energy cut-off E_2 of about 150 eV for Al and about 300 eV for Nb.

3.1. Band structures

3.1.1. Al. Shown in figure 1 are several calculations of the band structure for Al. We computed the bands using various numbers of PAOs and compare them with the more rigorous plane-wave result to give an indication of the importance of individual orbital components in the wavefunction. The potentials for each of these calculations are independently and self-consistently determined. We used a lattice constant of 4.03 Å. In figure 1(*a*) the band structure is computed using only sp³ orbitals with no supplementing low-energy plane waves. Remarkably, we find that, even with this small *a* basis, the lowest band is quite well reproduced. It is clear, however, that the sp³ PAOs do not produce a good overall band structure for Al. As expected, the error in the sp³ energies become increasingly worse as we move from the more localised lower-energy bands to the more extended higher-energy (excited) bands. Nevertheless, in view of the fact that they were calculated with only a 4 × 4 Hamiltonian matrix (compared with an approximate 70 × 70 plane-wave matrix), the sp³ bands seem surprisingly accurate, indicating that the PAOs are close to optimum for this material.

When a few low-energy plane waves are added to the sp³ basis (denoted sp³ + PW) (five to eight plane waves are added depending on the k point [20]), the bands are significantly improved (figure 1(b)). The addition of the few free-electron-like plane waves to the sp³ PAOs appears to have removed most of the discrepancy between the sp³
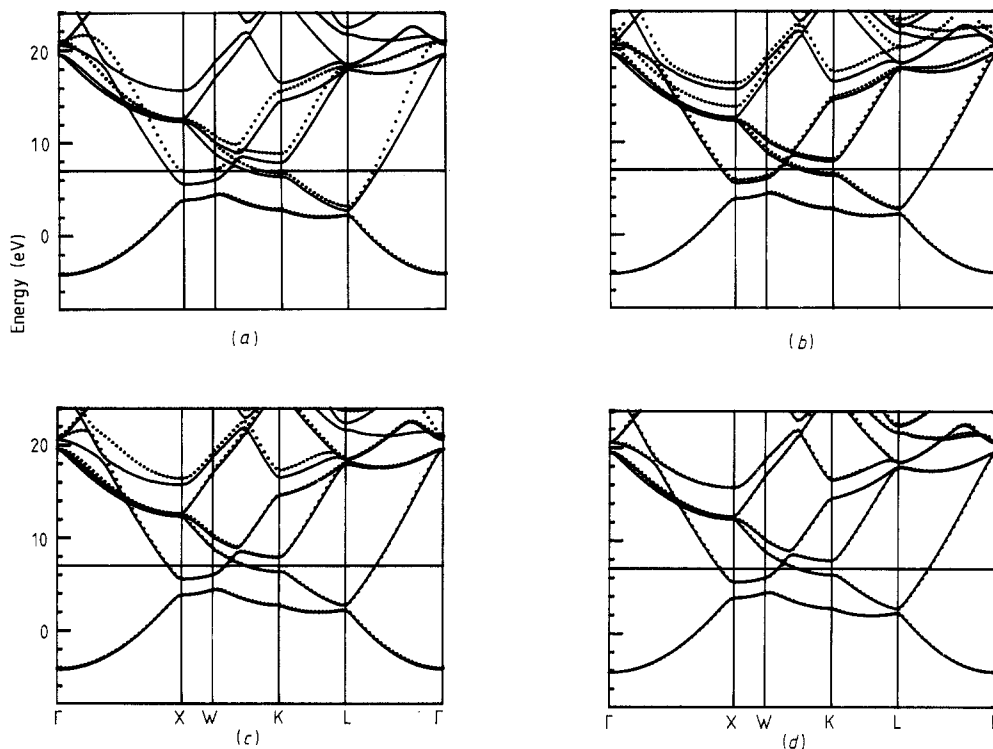
Figure 1. Comparison between pseudo-atomic band structures ($\cdots\cdots$) and the more rigorous plane-wave-derived band structures (———) for Al. The PAO approximations to the plane wave results shown are (*a*) sp^3, (*b*) sp^3 + PW (a plane-wave cut-off energy E_1 of 30 eV was used, which gives five to eight low-energy plane waves depending on the *k*-point), (*c*) sp^{3}d^5 and (*d*) sp^{3}d^5 + PW. We find all PAO approximations adequately represent the lowest band in Al, but excited d orbitals are needed to reproduce the half-filled band or higher-energy bands for this simple metal. No shifts of any kind were made in the bands.

bands and the pure plane-wave bands near the Fermi level. There are still, however, significant errors in the higher-energy bands for the sp^3 + PW calculation†.

If d orbitals are used (figure 1(*c*) and 1(*d*)), we see dramatic improvements in all bands. The use of d orbitals, however, more than doubles the Hamiltonian and overlap set-up time, making the calculations much longer. Even so, for even the most sophisticated orbital calculation which uses sp^{3}d^5 + PW(figure 1(*d*)), the method is still far faster, even for the perfect crystal, than a conventional plane-wave-only calculation, and the accuracy is virtually the same when highly excited states are unimportant. For defect systems where large unit cells are used, this speed-up becomes increasingly important, typically reducing overall computational effort by an order of magnitude or more.

† The number of plane waves in the basis is determined by the cut-off energy $E_1 = \hbar^2 |\mathbf{k} - \mathbf{g}_1|^2/2m$ and thus is dependent on the *k*-point. Plane waves not explicitly added to the low-energy plane-wave basis are contained as Fourier components in the expansion of the PAOs. Thus, discontinuities in the bands, which one might expect to arise owing to abrupt changes in the number of plane waves used for different *k*-points, do not appear.
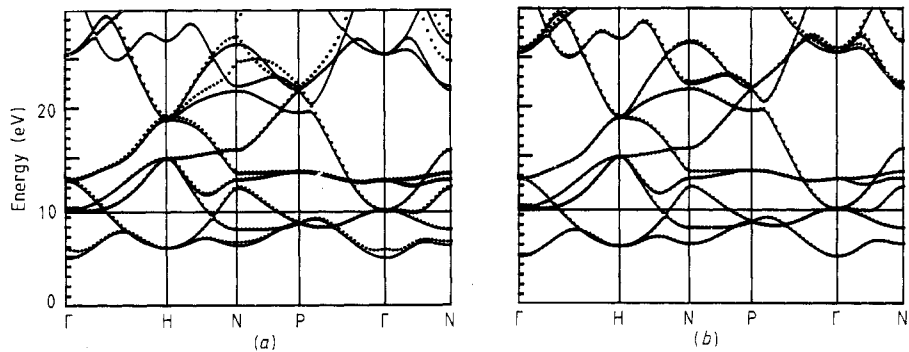
Figure 2. Comparison between pseudo-atomic band structures ($\cdots\cdots$) and the more rigorous plane-wave-derived band structures (———) for Nb. The PAO approximations to the plane-wave results shown are (a) sp^{3}d^5 and (b) sp^{3}d^5 + PW (a plane-wave cut-off energy E_1 of 50 eV was used, which gives 12 to 16 low-energy plane waves depending on the k-point). The delocalised s-like band (bottom band) is not as well represented by the localised functions especially around high-symmetry k-points in (a). Errors in this band and higher-energy bands are virtually eliminated by the introduction of just a few low-energy plane waves as in (b). No shifts of any kind were made in the bands.

3.1.2. Nb. In figure 2 we compare the band structures of Nb computed using sp^{3}d^5 PAOs (figure 2(a)) and sp^{3}d^5 PAOs supplemented with a few low-energy plane waves (sp^{3}d^5 + PW; see figure 2(b)), with that computed using a pure plane-wave basis. The lattice constant used here was 3.3 Å. Except for the lowest s-like band, we find that the overall agreement for the sp^{3}d^5 PAO calculation is already quite good. In the solid the atomic s states become highly extended and are therefore not well represented by a basis constructed from the atomic s orbitals. The pure orbital-based calculation (figure 2(a)) of the lowest band, which is derived mostly from the atomic s states, is therefore not well represented especially near high-symmetry k-points. As expected, the bands that lie near the Fermi level, which are derived from the more localized d states, are much better represented by the atomic basis than are the s levels. As with Al, the errors in the Nb bands, due to the use of orbitals, can again be nearly eliminated by the introduction of just a few (12–16) low-energy plane waves (figure 2(b)). Previous Gaussian orbital-based calculations [4] neglected the s and p-localised orbital functions and included only d functions. Without these more extended s and p functions, however, a significant number of plane waves had to be employed which may be undesirable for large systems.

3.2. Total energies

To study the method's total energy capability, we have also calculated the bulk lattice constants and bulk moduli for Al and Nb. We compare our PAO results using a number of PAO approximations with those of pure plane waves and with experiment in table 1. The bulk modulus $B(\approx a^{-1}\,\mathrm{d}^2E/\mathrm{d}a^2)$ is strongly dependent on the precise value of the lattice constant a used in its evaluation. Here we have consistently used the theoretically predicted value. We have also used a constant number of plane waves in the wavefunction expansion instead of a constant energy cut-off with lattice constant. This avoids the discontinuous jumps in the total energy as a plane wave is removed or added to the expansion but has the effect of underestimating lattice constants and overestimating bulk moduli for finite expansions when compared with the *true theoretical* value.

Table 1. Predicted lattice constants a and bulk moduli B for Al and Nb using sp^3, sp^3 + PW, sp^3d^5 PAOs and sp^3d^5 + PW compared with conventional plane-waves-only calculations and experimental values.

	Al		Nb	
	a (Å)	B (GPa)	a (Å)	B (GPa)
sp^3	4.25	50.1		
sp^3 + PW	4.12	61.5		
sp^3d^5	4.05	80.9	3.26	215.6
sp^3d^5 + PW	4.01	84.7	3.25	201.2
PW only	4.01	84.6	3.25	201.1
Experiment	4.03 [19]	72.2 [18] 76.0 [19]	3.30 [19]	170.2 [18]

We find that our results are in overall good agreement with experiment [18, 19] even when no low-energy plane waves are included in the basis. The greatest errors in Al again occur for the extreme case of only sp^3 PAOs. This small basis appears to be inadequate for Al, indicating that d-state hybridisation is important for the half-filled band. Adding a few (five to eight) plane waves only partially removed the problem.

When d orbitals are added to the basis, the discrepancies for Al are severely reduced. The d orbitals (4d) are of course necessary for Nb since they are valence orbitals. We see from table 1 that the greatest portion of the errors in the sp^3d^5 or sp^3d^5 + PW quantities do not appear to be associated with the use of localised orbitals since similar errors are present in the plane-wave calculations. As with the band structures, the values for the Al and Nb lattice constants and bulk moduli obtained using sp^3d^5 + PW are seen to be virtually identical with the plane-wave values. These errors of about 1% in the lattice constant and about 10% in the bulk modulus for the fully converged calculations are typical of all self-consistent LDA calculations.

4. Vacancy and self-interstitial in Al

Accurate calculation of defect formation energies in metallic systems is a problem of considerable difficulty, owing partly to the high sensitivity of these quantities to electron rearrangement and screening effects. Charge densities in the vicinity of a defect may be severely altered from that of the perfect metal. Hence, a significant amount of variational freedom is required for a reliable calculation. This is especially true for vacancies and interstitials where the coordination number is changed.

In this section, we employ pseudo-atomic orbitals to calculate the undistorted vacancy and self-interstitial formation energies in Al. We approximate the isolated defect by a periodic array of defects using a simple cubic (SC) supercell with a volume containing 32 atomic sites. Smaller supercells are also used for comparison. The vacancy

formation energy $\varepsilon_{\text{form}}(V)$ and interstitial formation energy $\varepsilon_{\text{form}}(I)$ are obtained from the supercell total energies by

$$\varepsilon_{\text{form}}(V) = E(N - 1, V) - [(N - 1)/N]E(N)$$

and

$$\varepsilon_{\text{form}}(I) = E(N + 1, I) - [(N + 1)/N]E(N)$$

where N is the number of atomic sites in the supercell (equal to 32 for the largest cell), $E(N - 1, V)$ is the total energy for the $(N - 1)$-atom vacancy supercell, $E(N + 1, I)$ is the total energy for the $(N + 1)$-atom interstitial supercell and $E(N)$ is the perfect-crystal supercell energy. The lattice constant (of 2×4.03 Å $= 8.06$ Å for the 32-atom cell) was held fixed for both the perfect-supercell and the defect-supercell calculations. Our definition for the vacancy formation energy, which assumes a constant volume, differs slightly from that used in earlier work [20], where a constant density was assumed. Although in the limit of an infinite supercell both definitions must converge to the same expression, it is debatable which should be used for the practical case where cells of finite size must be employed.

The total energy calculations were done using an sp^3d^5 PAO basis on each atom in the supercell (and also on the vacancy site for the vacancy calculation) along with a few low-energy plane waves. The plane-wave kinetic-energy cut-off E_1 ($=\hbar^2\text{g}_1^2/2m$ in equation (3)) and the local-orbital plane-wave expansion cut-off E_2 used were 30 eV and 120 eV, respectively. Through tests on the smallest supercell, the low-energy plane-wave cut-off of 30 eV was determined to be high enough to make our PAO results agree to within about 0.01 eV with those of a 120 eV full plane-wave calculation. We thus expect the accuracy to be sufficient for the larger supercells as well. For the 32-site supercell, we used four special k-points in the irreducible (one forty-eighth) Brillouin zone. To obtain a formation energy, considerable precision must be maintained throughout every aspect of the calculation. Small errors per atom can become significant if introduced into every cell of a large supercell. We have thus made extensive convergence checks on all quantities affecting the total energy. The overall error of our calculation due to k-point, basis-set and self-consistency convergence was at most of the order of 0.1 eV, which was considered acceptable in view of the fact that other errors associated with the pseudopotential–supercell method itself are expected to be worse.

5. Results

The values obtained for the formation energy of the vacancy in Al and the self-interstitial in Al were 0.52 eV and 10.21 eV, respectively. The relatively high value for the interstitial formation energy may account for the apparent lack of experimental measurements of its energetics; we could find no experimental value for the Al self-interstitial formation energy. We expect the theoretical value for the interstitial formation energy to be reduced considerably if relaxation were included but it will, in any case, remain high in comparison with the vacancy formation energy. The vacancy formation energy has been experimentally determined to be 0.66 eV [21] which, in the light of numerical uncertainties, is in good agreement with our theoretical prediction.

A major concern related to the use of supercells is the effect due to spurious interactions between neighbouring defects. These errors are usually quite unpredictable and may bring into question the reliability of the results. To check cell size convergence
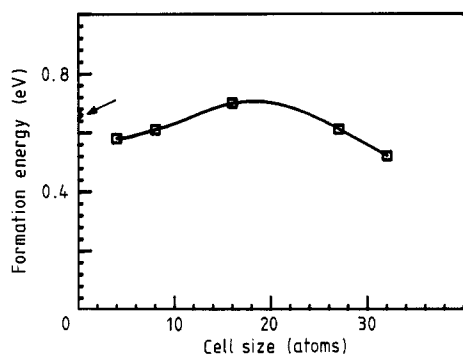
Figure 3. Relationship between the supercell size and the corresponding formation energy for an Al vacancy. The largest supercell consisted of 32 sites and represents the best calculation of the formation energy (0.52). Remarkably, however, we see no large deviations in the formation energy from the experimental value even when the formation energy was computed using unrealistically small (four-atom) supercells, where defect interactions must obviously be present. Apparently, such interactions introduce errors which largely cancel for the case of Al. Arrow: experiment.

and to investigate the nature of this defect-overlap effect, we have therefore computed the formation energy using several different supercell sizes. The supercells that we considered were four-site SC, eight-site FCC, 16-site BCC, 27-site FCC and 32-site SC. To ensure that meaningful comparisons could be made, the same basis set, energy cut-offs and k-point densities were maintained in all supercells. The results for the vacancy formation energy against supercell size are shown in figure 3. We find the deviations in the formation energies between different-sized cells is remarkably small, being less than 0.2 eV for all supercells considered. The unrealistically small four-site supercell, in fact, gives a nearly identical formation energy as the largest 32-site cell. This unexpected behaviour may be peculiar to simple metals such as Al, where charge can easily rearrange without upsetting the basic character in the structure of the bands near the Fermi level. The surprising stability of our predicted formation energies with respect to supercell size is an indication that keeping the volume fixed, as we did, may be more realistic than attempting to keep a constant density by shrinking the vacancy supercell. In general, the appropriateness of such a volume modification is questionable since it biases the total energy either higher or lower depending only on the relative positions of the theoretical lattice constant and that used in the calculation. For the pseudopotential used here, for example, shrinking the volume of the vacancy supercell slightly would automatically introduce an unphysical negative-energy component into the vacancy formation energy, simply because our predicted lattice constant is too small compared with the experimental value used in the perfect-crystal supercell calculation. If, on the contrary, the theoretical value were used, such as was done in [20], then a small positive-energy component would be introduced into the (shrunken) vacancy supercell total energy. It is not surprising therefore that the value for the vacancy formation energy obtained in [20] (1.5 eV) was higher than that predicted here, although the difference of nearly an electronvolt is perhaps more than expected.

To investigate pseudopotential effects further, we have also calculated the vacancy formation energy in Al using the pseudopotential from [15] for Al. This pseudopotential, in either of the two largest supercells, was found to give a formation energy of about 1.0 eV, which is midway between the result for our pseudopotential and that used in [20]. It thus appears that these energies are quite sensitive to small differences in pseudopotentials, so that errors in formation energies of the order of 0.5 eV should probably be expected, at least for metals. We suspect that this effect due to differences in pseudopotentials may have combined with other effects due to differences in supercell sizes, cut-off energies and the difference in definition, to produce the discrepancy found

between our results and those in [20]. In any case, we do not believe the discrepancy is related to the use of pseudo-atomic orbitals.

6. Conclusion

We have shown that pseudo-atomic orbitals optionally supplemented with a few low-energy plane waves form an efficient basis for the calculations of electronic structure and total energies in metals. Both free-electron-like (plane-wave) and localised (orbital) components of the wavefunction can be well described by this method. We have shown that our PAO results compare favorably with plane-wave results and with experiment for the bulk band structure, lattice constants and bulk moduli. We have also used pseudo-atomic orbitals to calculate the vacancy and self-interstitial formation energies in Al. The method has the appealing aspects of being easily interpretable in terms of a few interacting atomic orbitals and seems to be computationally much faster than other first-principles methods. The latter point makes the PAO method particularly attractive for dealing with systems in large supercell configurations.

Acknowledgments

References ·

[1] Jansen R W and Sankey O F 1987 *Phys. Rev.* B **36** 6520
[2] Jansen R W and Sankey O F 1987 *Solid State Commun.* **64** 197; 1988 *J. Appl. Phys.* **64** 2415
    Sankey O F and Jansen R W 1988 *J. Vac. Sci. Technol.* B **6** 1240
[3] Louie S G, Ho K-M and Cohen M L 1978 *Phys. Rev.* B **19** 1774
    Chelikowsky J R and Louie S G 1984 *Phys. Rev.* B **29** 3470
[4] Fu C-L and Ho K-M 1983 *Phys. Rev.* B **28** 5480
[5] Wang C S and Klein B M 1981 *Phys. Rev.* B **24** 3393, 3417
[6] Pederson M R 1988 *Phys. Rev.* B **37** 10319
[7] Feibelman P J 1986 *Phys. Rev.* B **33** 719
[8] Kasowski R V, Tsai M-H, Rhodin T N and Chambliss D D 1986 *Phys. Rev.* B **34** 2656
[9] Lafon E E and Lin C C 1966 *Phys. Rev.* **152** 579
[10] Krakauer H, Posternak M, Freeman A J and Koelling D D 1981 *Phys. Rev.* B **23** 3859
[11] Ihm J, Zunger A and Cohen M L 1979 *J. Phys. C: Solid State Phys.* **12** 4409
[12] Andersen O K 1975 *Phys. Rev.* B **12** 3060
[13] Williams A R, Kubler J and Gelatt C D, Jr 1979 *Phys. Rev.* B **19** 6094
[14] Hamann D, Schluter M and Chiang C 1979 *Phys. Rev. Lett.* **43** 1494
[15] Bachelet G B, Hamann D R and Schluter M 1982 *Phys. Rev.* B **26** 4199
[16] Perdew J and Zunger A 1981 *Phys. Rev.* B **23** 5048
[17] Ceperley D M and Alder G J 1980 *Phys. Rev. Lett.* **45** 566
[18] Ashcroft N W and Mermin N D 1976 *Solid State Physics* (Philadelphia, PA: Holt, Rinehart and Winston)
[19] Kittel C 1987 *Introduction to Solid State Physics* (New York: Wiley)
[20] Chakraborty B and Siegel R W 1983 *Phys. Rev.* B **27** 4535
[21] Berger A S, Ockers S T and Siegel R W 1978 *J. Nucl. Mater.* **69–70** 734
    Fluss M J, Smedskjaer L C, Chason M K, Legnini D G and Siegel R W 1978 *Phys. Rev.* B **17** 3444